Estimation of Respiratory Rates Using the Built-in Microphone of a Smartphone or Headset

Yunyoung Nam, Bersain A. Reyes, *Student Member, IEEE*, and Ki H. Chon, *Senior Member, IEEE*

***Abstract*—This paper proposes accurate respiratory rate estimation using nasal breath sound recordings from a smartphone. Specifically, the proposed method detects nasal airflow using a built-in smartphone microphone or a headset microphone placed underneath the nose. In addition, we also examined if tracheal breath sounds recorded by the built-in microphone of a smartphone placed on the paralaryngeal space can also be used to estimate different respiratory rates ranging from as low as 6 breaths/min to as high as 90 breaths/min. The true breathing rates were measured using inductance plethysmography bands placed around the chest and the abdomen of the subject. Inspiration and expiration were detected by averaging the power of nasal breath sounds. We investigated the suitability of using the smartphone-acquired breath sounds for respiratory rate estimation using two different spectral analyses of the sound envelope signals: The Welch periodogram and the autoregressive spectrum. To evaluate the performance of the proposed methods, data were collected from ten healthy subjects. For the breathing range studied (6–90 breaths/min), experimental results showed that our approach achieves an excellent performance accuracy for the nasal sound as the median errors were less than 1% for all breathing ranges. The tracheal sound, however, resulted in poor estimates of the respiratory rates using either spectral method. For both nasal and tracheal sounds, significant estimation outliers resulted for high breathing rates when subjects had nasal congestion, which often resulted in the doubling of the respiratory rates. Finally, we show that respiratory rates from the nasal sound can be accurately estimated even if a smartphone's microphone is as far as 30 cm away from the nose.**

***Index Terms*—Nasal sound, respiratory rate estimation, smartphone, sound intensity, tracheal sound.**

I. Introduction

RESPIRATION rate (RR) is one of the key vital signs, but it is not possible to obtain it in a manner that is reliable, readily-available, cost effective, and easy to use by the general public [1]. The lack of a reliable and readily available RR measurement is one of the major contributors to avoidable adverse events. A retrospective study of more than14 000 cardiopulmonary arrests in acute care hospitals showed that 44% were respiratory in origin [2]. In addition, a study by Health Grades showed that respiratory failure, a key Patient Safety Indicator, has increased in U.S. Acute Care Hospitals. The reported incidence is 17.4 per 1000 hospital admissions leading to over 15 000 avoidable deaths at a cost to the healthcare system of more than $1.8 billion [3]. Moreover, the continuous monitoring of RR as an indicator of ventilation is particularly important for patients in the intensive care unit [4].

The most common method for measuring RR consists of either manually counting the chest wall movements or auscultation of breath sounds with a stethoscope. Previous studies have shown that these manual methods tend to be unreliable in acute care settings and are limited by their intermittent cadence [5]. For automated approaches to RR assessment, sensors that measure airflow are often used in clinical settings. The airflow is usually measured by spirometry devices and some of the popular sensors include pneumotachograph or nasal cannulae that are connected to a pressure transducer, heated thermistor, or anemometer. Although the spirometry devices provide accurate estimates of RR, breathing through a mouthpiece or facemask connected to a pneumotachograph is inconvenient and adds unnecessary airway resistance. More importantly, due to high cost, inconvenience for patients' everyday use, and immobility of the traditional spirometry devices, this is impetus for developing simple, cost effective, and portable devices for estimating RR [4].

One approach has the potential to meet the above criteria for easily accessible, affordable, and on-demand monitoring of RR via the use of smartphones without any external sensors. We have recently shown that the good estimates of resting RR can be obtained directly from a finger's pulsatile light intensity fluctuations which are captured using the smartphone's built-in camera [6]. However, the accuracy of this approach for RR estimation degrades when breathing rates are higher than 30 breaths/min. To mitigate this limitation, we propose in this paper to use either a built-in microphone or the microphone of a headset plugged to a smartphone to estimate the RR over a wide dynamic range.

The Stethoscope is a common device routinely used by physicians to determine the health status of the respiratory system. Given that a stethoscope is essentially a microphone, it should be expected that a microphone can also be used to obtain RR [7], [8]. A key technical challenge is to discriminate between inspiratory and expiratory sound signals so that a correct RR can be determined. Fortunately, dynamics of the inspiration and expiration are different, hence, many different approaches can be used [9]–[12] to discriminate between the two phases of the breathing cycle. Some of the noted automated approaches for respiratory rate estimation include estimating the intensity changes of breathing sounds [13], the relative changes of the total sound

Manuscript received March 3, 2015; revised June 9, 2015 and July 28, 2015; accepted September 18, 2015. Date of publication September 22, 2015; date of current version December 6, 2016. This work was supported by the Soonchunhyang University Research Fund. This work was also supported by the US Army Medical Research and Materiel Command (USAMRMC) under Grant No. W81XWH1210541.

Y. Nam is with the Department of Computer Science and Engineering, Soonchunhyang University, Asan 336-745, Korea (e-mail: ynam@sch.ac.kr).

B. A. Reyes and K. H. Chon are with the Department of Biomedical Engineering, University of Connecticut, Storrs, CT 06269 USA (e-mail: bersain.reyes@uconn.edu; kchon@uconn.edu).

Color versions of one or more of the figures in this paper are available online at http://ieeexplore.ieee.org.

Digital Object Identifier 10.1109/JBHI.2015.2480838

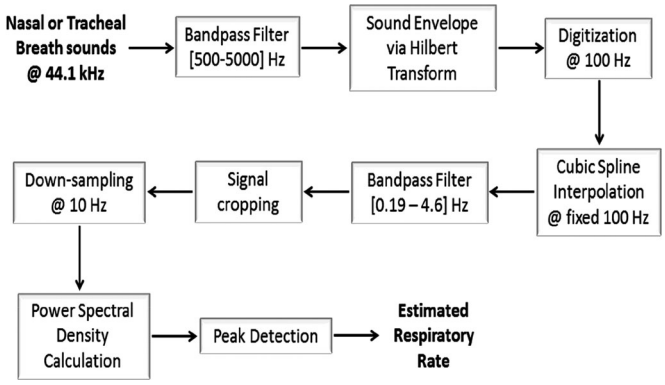

Fig. 1. Flowchart of the proposed method for respiratory rate estimation using smartphone acquired tracheal and nasal breath sounds.

power [14], the analysis of the tracheal sound entropy [15], and bioacoustic analysis [10]. While expiratory sounds recorded at the trachea are slightly louder than inspiratory sounds [16], in general the dynamic characteristics of inspiration are similar to expiration sounds recorded at the trachea. In contrast, the intensities of nasal breath sounds recorded near a subject's nose during inspiration and expiration are different. Hence, by taking an advantage of different acoustic properties of respiration sounds measured at either trachea or nose, and with a built-in smartphone microphone or the microphone of a headset cabled to a smartphone, we developed an approach to estimate the RR that is accurate for a wide dynamic range from 6 breaths/min to 90 breaths/min. The aim of the paper is to show that our method allows a reliable determination of the RR without any external sensors, but by utilizing only the built-in microphone or headset microphone of a smartphone.

II. Materials and Methods

A. Data Acquisition

Data were collected from ten healthy nonsmoking volunteers with ages ranging from 20 to 40 years. The experimental protocol was approved by the Institutional Review Board of Worcester Polytechnic Institute and all volunteers signed the informed consent prior to data acquisition.

Data were collected while volunteers were seated in the upright position in a regular office room. Tracheal and nasal breathing sound signals were recorded by a built-in microphone and the headset microphone of an iPhone 4S (Apple, Inc., Cupertino, CA, USA) placed on the subject's suprasternal notch on the neck and the philtrum under the nose, respectively. For tracheal breath sound recording, the built-in microphone was manually kept in a fixed position by the subject, while for nasal breathing sound recording, the headset's microphone was placed gently under the subject's nose to assure that it would not be displaced during the experiment. None of the subjects reported any discomfort with the microphone placement.

For determining true breathing rates, inductance plethysmography bands were placed around the subject's chest and abdomen (Respitrace, Ambulatory Monitoring, Inc., Ardsley, NY, USA). These reference signals were acquired and stored in a personal computer using LabChart 7 software (ADInstruments, Inc., Dunedin, New Zealand) at a sampling rate of 400 Hz. Breathing sound data from microphones were collected directly to an iPhone using 16-bits per sample with a sampling rate of 44 100 Hz. In addition to collecting sound signals, the amplitude of their envelope was also computed and stored on the smartphone.

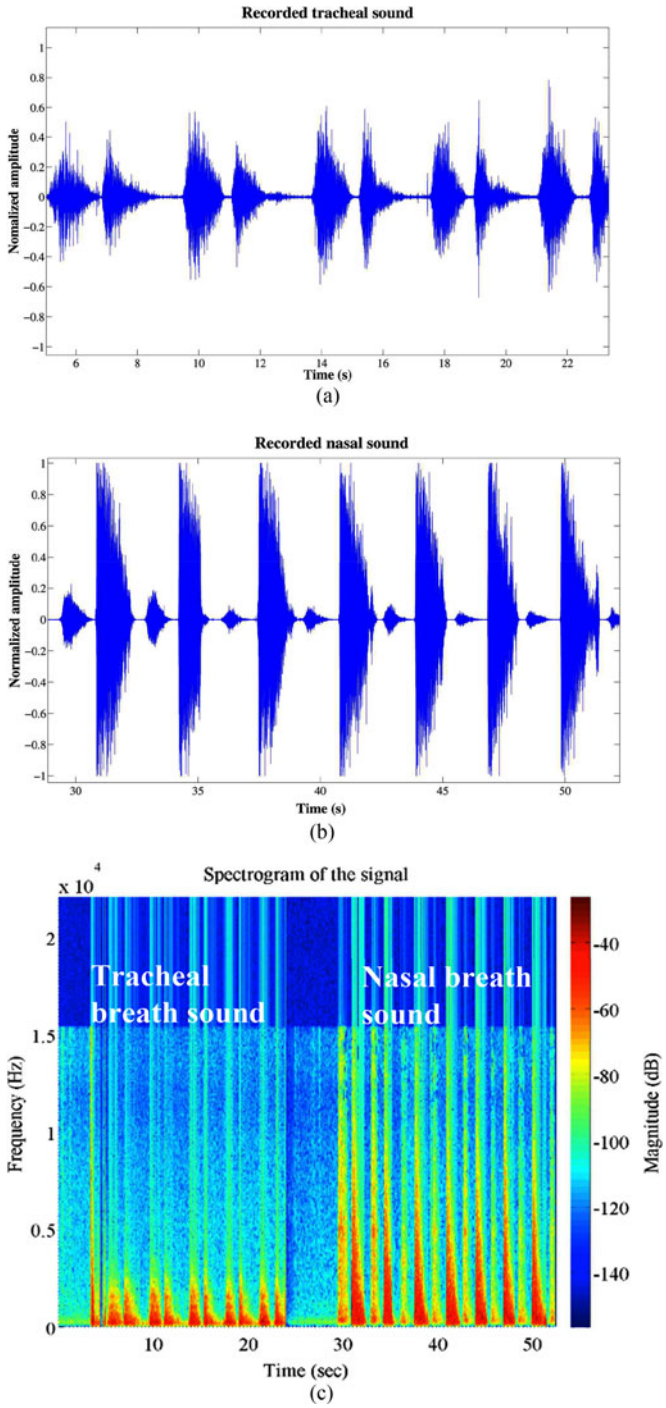

Fig. 2. Examples of recorded tracheal and nasal breath sound. (a) Recorded tracheal signal using the built-in microphone. (b) Recorded nasal signal using the earpiece microphone. (c) Sound spectrogram.

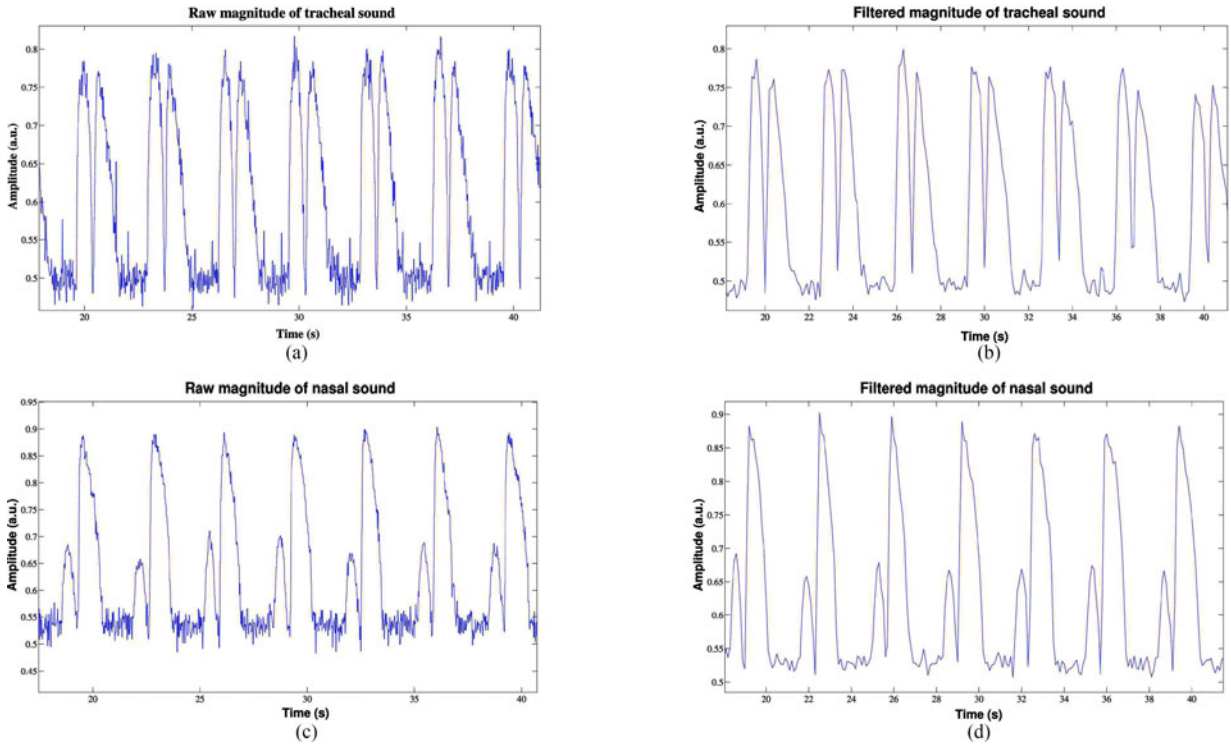

Fig. 3. Typical recorded tracheal and nasal sound envelope signals. (a) Raw envelope of tracheal sound. (b) Filtered envelope of tracheal sound signal. (c) Raw envelope of nasal sound. (d) Filtered envelope of nasal sound.

First, the audio signals were band-pass filtered in the range of 500–5000 Hz to remove the effects of low-frequency and high-frequency noise. The Hilbert transform was used to extract the envelope of the filtered sound signal. For a continuous-time signal *x(t)*, its Hilbert transform is defined as follows [17]:

$$H\left(x\left(t\right)\right) = \frac{1}{\pi}\int_{-\infty}^{\infty} x\left(\tau\right)\frac{1}{t-\tau}d\tau. \tag{1}$$

The amplitude of the envelope was calculated as the magnitude of its analytic signal, i.e., complex valued. The resulting signal was then digitized and stored in the smartphone for further processing offline. The amplitude of the envelope was digitized at a rate of 100 Hz. These envelope signals were digitized at this lower rate to reduce computational time and data capacity, and mainly because the highest breathing rate we were concerned with was at most 2 Hz.

All subjects were instructed to breathe at a metronome rate according to a timed beeping sound programmed at a given frequency. Each subject was wearing earphones and was asked to inhale at each beep sound followed by exhalation before the next beep sound occurred. Data were collected for breathing frequencies ranging from 0.1 to 1.5 Hz at increments of 0.1 Hz, which corresponds to breathing rates ranging from 6 to 90 breaths/min at steps of 6 breaths/min. Prior to data collection, all subjects were acclimated to the different metronome breathing rates. For each subject, 3 min of breathing data were collected at each programed metronome frequency. For breathing rates greater than 60 breaths/min, subjects were given ample time break before the start of the next breathing rates.

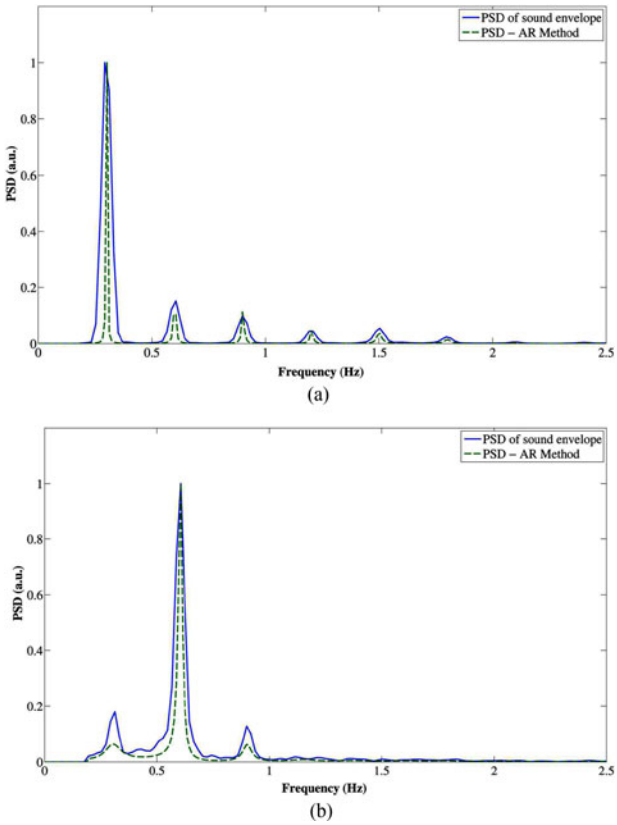

Fig. 4. PSD examples of nasal sounds using envelope and AR model approaches. (a) Normal nasal breathing at frequency rate of 0.3 Hz. (b) Nasal breathing with nasal obstruction at frequency rate of 0.3 Hz.

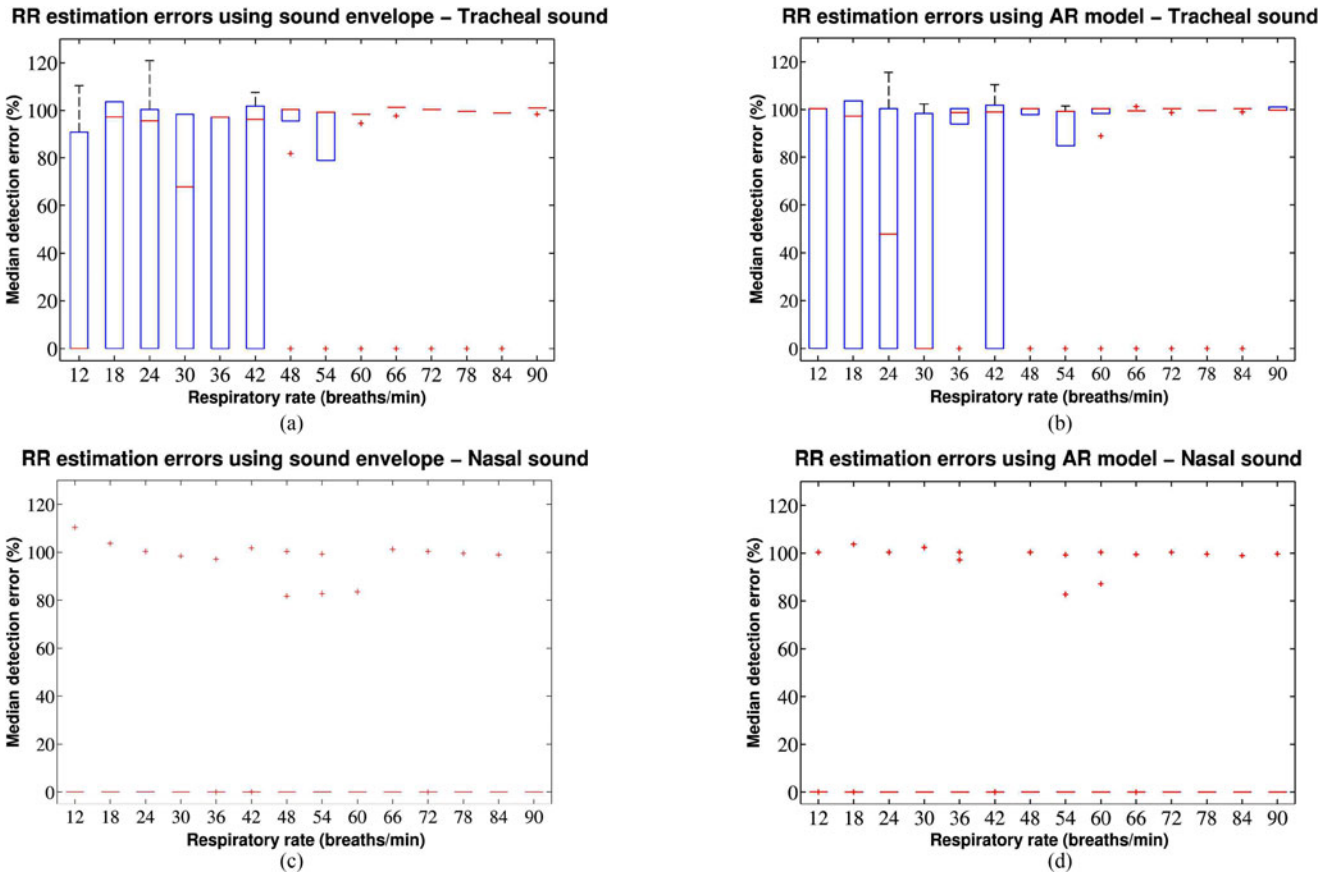

Fig. 5. Median and IQR respiratory rate estimation errors ε measured from the respiratory rate results calculated by the maximum peak in PSDs from (a) tracheal breath sound, (b) AR model of tracheal breath sound, (c) nasal breath sound, and (d) AR model of nasal breath sound.

B. Preprocessing

The smartphone's sampling frequency was not constant but varied around 100 Hz, therefore, a cubic spline algorithm was used to interpolate the digitized signals to a constant 100 Hz. Finally, the smoothed envelope signals were band-pass filtered between 0.19 and 4.6 Hz, using a rectangular window in the frequency domain, and then downsampled from 100 to 10 Hz. After this downsampling, the initial and final 10 s of the recordings were discarded. This preprocessing was performed on a personal computer using MATLAB (R2012a, The Mathworks, Inc., Natick, MA, USA).

C. Data Analysis

In order to determine the appropriate respiratory rate, the power spectrum of the preprocessed tracheal and nasal sound envelopes were investigated using two different methods: 1) the Welch periodogram technique and 2) the autoregressive (AR) power spectral analysis technique via the Burg algorithm. In the first approach, the PSD of each segment was computed via Welch periodogram. In the second approach, the Burg method was used to estimate the AR coefficients from the sampled data by the simultaneous minimization of the forward and backward linear prediction squared errors, while the AR coefficients were constrained to satisfy the Levinson–Durbin recursion. An AR model order of 50 was employed based on the minimum description length criterion [18].

The respiratory rate can be calculated by either the largest peak of PSDs of the sound envelope or via the AR model of a sound envelope. The true RR was found by computing the PSD of the reference respiration signal and finding the frequency at which its maximum spectral peak occurred. In general, the average error of the respiratory rate estimation based on the maximum spectral peak of PSD was larger for the high-frequency breathing rates. The respiratory frequency can be determined by the frequency corresponding to the maximum peak of PSD, provided that the frequency spectra of inspiration and expiration are similar. However, they become different when subjects have nasal congestion, for example. When this occurs, the respiratory rates can be (incorrectly) double.

The estimated RR from the smartphone's microphone was compared to the true RR acquired from the Respitrace system to test the reliability and accuracy of the proposed method. For each respiratory rate, detection errors were found for all subjects using the two different spectral methods as previously described. The respiratory rate estimation error ε was calculated for each

TABLE I
ACCURACY AS DETERMINED BY MEDIAN ERRORS AND IQR MEASURED FROM THE RESPIRATORY RATE RESULTS OBTAINED FROM NASAL BREATHING SOUND SIGNAL ($N = 10$)

Respiration Rate	Respiration Rate	Estimation Error	Sound envelope		AR model of sound envelope	
Breaths/min (beep sound)	Breaths/min (bands)	ε	Tracheal sound	Nasal sound	Tracheal sound	Nasal sound
6 (0.1 Hz)	6.055(0.101 Hz)	Median	90.821 ± 18.775	111.306 ± 95.292	58.518 ± 136.685	0.3 ± 42.535
		IQR	40.969 ± 19.313	119.823 ± 52.329	85.394 ± 35.133	90.768 ± 42.73
12 (0.2 Hz)	13.184 (0.22 Hz)	Median	97.148 ± 45.796	0.055 ± 33.108	29.909 ± 13.734	0.064 ± 40.132
		IQR	96.241 ± 46.047	0 ± 0	98.998 ± 46.61	25.084 ± 11.824
18 (0.3 Hz)	18.164 (0.303 Hz)	Median	101.792 ± 46.731	0.055 ± 31.087	101.792 ± 47.34	0.008 ± 31.1
		IQR	100.391 ± 29.857	0 ± 0	100.391 ± 39.924	0.012 ± 0.005
24 (0.4 Hz)	23.965 (0.399 Hz)	Median	8.278 ± 3.903	0.055 ± 30.1	26.921 ± 12.691	0 ± 30.117
		IQR	99.307 ± 38.951	0.01 ± 0.004	99.307 ± 39.146	0 ± 0
30 (0.5 Hz)	29.883 (0.498 Hz)	Median	40.163 ± 18.933	0.024 ± 29.526	35.748 ± 16.852	0.002 ± 30.707
		IQR	98.444 ± 29.427	0 ± 0	100.391 ± 29.794	0 ± 0
36 (0.6 Hz)	35.918 (0.599 Hz)	Median	0.959 ± 0.452	0.008 ± 29.143	4.31 ± 2.032	0.005 ± 39.514
		IQR	101.282 ± 30.284	0.012 ± 0.005	99.503 ± 29.915	24.29 ± 11.45
42 (0.7 Hz)	42.305 (0.705 Hz)	Median	0.886 ± 0.417	0.002 ± 30.534	0 ± 0	0.002 ± 0.031
		IQR	100.391 ± 30.116	0.026 ± 0.012	100.391 ± 30.067	0.002 ± 0.001
48 (0.8 Hz)	47.93 (0.799 Hz)	Median	0 ± 0	0 ± 36.67	0.406 ± 0.191	0 ± 40.155
		IQR	99.64 ± 29.891	20.444 ± 9.637	99.64 ± 29.892	25.107 ± 11.836
54 (0.9 Hz)	53.73 (0.896 Hz)	Median	0 ± 0	0 ± 36.598	0 ± 0	0 ± 36.6
		IQR	98.998 ± 29.699	20.731 ± 9.773	100.391 ± 30.074	20.701 ± 9.759
60 (1.0 Hz)	59.766 (0.996 Hz)	Median	0 ± 0	0.002 ± 25.065	0.348 ± 0.164	0.002 ± 37.626
		IQR	101.044 ± 1.04	0 ± 0	99.74 ± 0.598	21.791 ± 10.272
66 (1.1 Hz)	66.152 (1.103 Hz)	Median	0.65 ± 0.307	0.003 ± 30.384	1.305 ± 0.615	0.001 ± 29.851
		IQR	97.148 ± 45.796	0 ± 0	29.909 ± 13.734	0.001 ± 0
72 (1.2 Hz)	72.072 (1.201 Hz)	Median	96.241 ± 46.047	0.005 ± 30.116	98.998 ± 46.61	0 ± 30.117
		IQR	101.792 ± 46.731	0.001 ± 0	101.792 ± 47.34	0 ± 0
78 (1.3 Hz)	77.93 (1.299 Hz)	Median	100.391 ± 29.857	0.004 ± 29.891	100.391 ± 39.924	0 ± 29.892
		IQR	8.278 ± 3.903	0 ± 0	26.921 ± 12.691	0 ± 0
84 (1.4 Hz)	83.79(1.397 Hz)	Median	99.307 ± 38.951	0.002 ± 29.699	99.307 ± 39.146	0.001 ± 29.699
		IQR	40.163 ± 18.933	0 ± 0	35.748 ± 16.852	0 ± 0
90 (1.5 Hz)	90.234 (1.504 Hz)	Median	98.444 ± 29.427	0.001 ± 0	100.391 ± 29.794	0.001 ± 39.896
		IQR	0.959 ± 0.452	0 ± 0	4.31 ± 2.032	24.935 ± 11.755

respiratory frequency

$$\varepsilon = \frac{\text{mean}\,(R - R_{est})^2}{\text{mean}\,(R)^2} \times 100 \qquad (2)$$

where R and R_{est} represent reference and estimated respiratory rate, respectively. The values of error were averaged for all subjects.

Fig. 1 shows the block diagram of the proposed method for estimating the respiratory rate from either the tracheal or nasal breath sounds acquired from a smartphone.

III. RESULTS

Fig. 2 shows a typical 20-s recording with a built-in microphone and an earpiece (headset) microphone together with their corresponding sound spectrograms. Fig. 2(a) and (b) shows the raw data of the tracheal and nasal breath sounds, respectively. Fig. 2(c) shows the sound spectrogram of tracheal and nasal breathing signals, where the vertical axis corresponds to the frequency and the horizontal axis to the time. Each color represents the power of the signal at a specific time and frequency, with the power decreasing from red to blue. For the tracheal sounds, inspiration and expiration tend to have similar frequency distributions. Note that more spectral power is observed in nasal breath sound than in tracheal breath sound. Also, the spectral power of inspiratory phases in nasal breath sound is less than that of their expiratory phases.

Examples of estimated envelope signals from recorded tracheal and nasal sounds are presented in Fig. 3. Typical unfiltered envelope signals from a built-in smartphone microphone and an earpiece-type headset's microphone are shown respectively in Fig. 3(a) and (c) while the postband-pass filtered and cubic spline interpolated envelope signals are shown in Fig. 3(b) and (d). Note that undesired sound activities are removed from the original signals. It can be seen that the filtered and splined magnitude signals follow the absolute values of flow signals, as has been reported by Que *et al.* [19]. Note that the amplitude of the estimated flow does not represent the actual amount of flow in L/s, as it is not calibrated.

Fig. 4 shows two different spectral estimates of the filtered sound envelope signals: the standard power spectrum and the AR model-based spectrum from a normal subject, shown in Fig. 4(a), and from a subject suffering nasal congestion, shown in Fig. 4(b), both when the breathing rate was 0.3 Hz. In these figures, the maximum peaks were obtained at the first- and the second-order harmonic frequencies, respectively. In general, the respiratory frequency can be determined as the frequency corresponding to the maximum peak of the PSD. However, the breathing rate of a subject suffering from nasal congestion was found to be doubled, as shown in Fig. 4(b).

Fig. 5 shows boxplots with the median and interquartile range (IQR) errors obtained from the respiratory rates calculated by the maximum peak in PSDs of tracheal sound envelope and AR spectrum of the tracheal sound envelope, shown in Fig. 5(a)–(b),

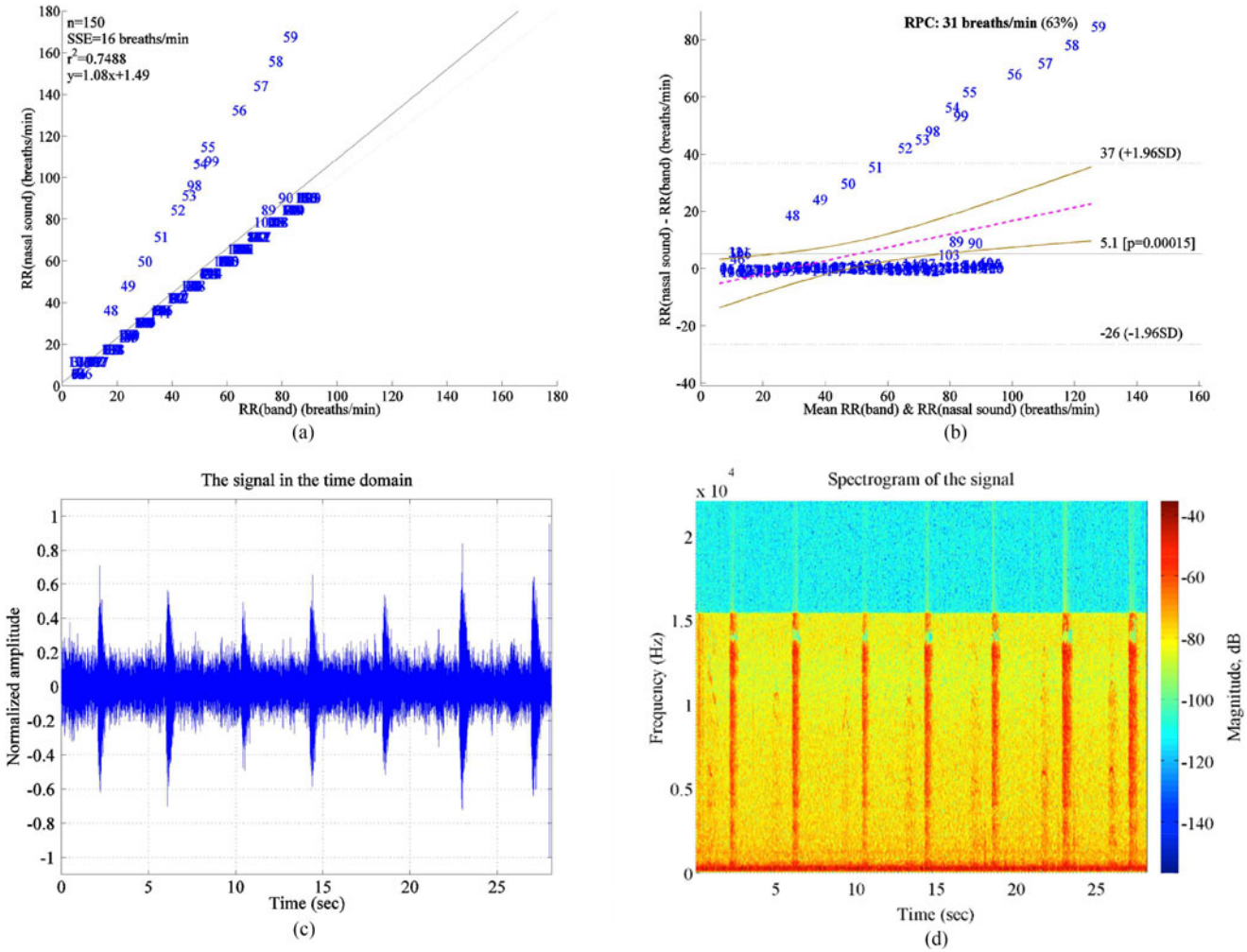

Fig. 6. Examples of Bland–Altman plot, correlation plot, and the recorded nasal breathing sound recorded with a built-in microphone of an iPhone 4S. (a) An example of a correlation plot. (b) An example of a Bland–Altman plot with proportional bias regression line. (c) Time waveform. (d) Spectrogram.

and the PSD of the nasal sound envelope and the AR spectrum of the nasal sound envelope, shown in Fig. 5(c)–(d). These figures indicate how well these two methods perform in estimating respiratory rates. The median and IQR of respiratory rate estimation errors were obtained from each reference and derived RR as defined in (2). The lower boundary of the box indicates the 25th percentile, a line within the box marks the median, and the upper boundary of the box indicates the 75th percentile. Whiskers (error bars) above and below the box indicate the 90th and 10th percentiles. Therefore, the area of the blue box is an indication of the spread, i.e., the variation in median error (or IQR), across the sample. Red crosses represent the outliers.

The respiratory rate estimation error ε was found to be lowest for nasal sound envelope and AR model from nasal sound envelope at all breathing rates as shown in Table I. The errors ε of sound envelope and AR model of nasal sound envelope were 7.43% and 0.025%, respectively. There was no significant difference in the average respiratory rate estimation error between the two approaches except for 0.1 Hz. As shown in Table I ($RR = 0.1$ Hz), it is difficult to detect low frequency component (envelope) because the signal-to-noise ratio decreases sharply at the low frequency band.

Fig. 6 shows the correlation and Bland–Altman plots with experiment numbers (1–150) for the mean RR data from nasal breathing signals and the inductance plethysmography bands, a typical 30-s nasal breathing sound signal obtained with the built-in microphone of an iPhone 4S, and its corresponding sound spectrogram. Similarly, Fig. 7 shows the raw data of the recorded nasal breathing sound during spontaneous breathing when the distance between the nose and iPhone was 30 cm.

In Fig. 7(a) and (b), inspiration and expiration were observed in both the sound signal and the magnitude signal. Fig. 7(c) contains peaks near 0.2539, 0.4883, and 0.7227 Hz. The real breathing rate was 0.2539 Hz. Finally, Fig. 8 shows examples of the recorded nasal breathing sound with background vocal noises during spontaneous breathing when the distance between nose and iPhone was 30 cm. Respiratory rate was measured by a peak near 0.3125 Hz as shown in Fig. 8(c). The real breathing rate was 0.3125 Hz as measured by the Respitrace system.

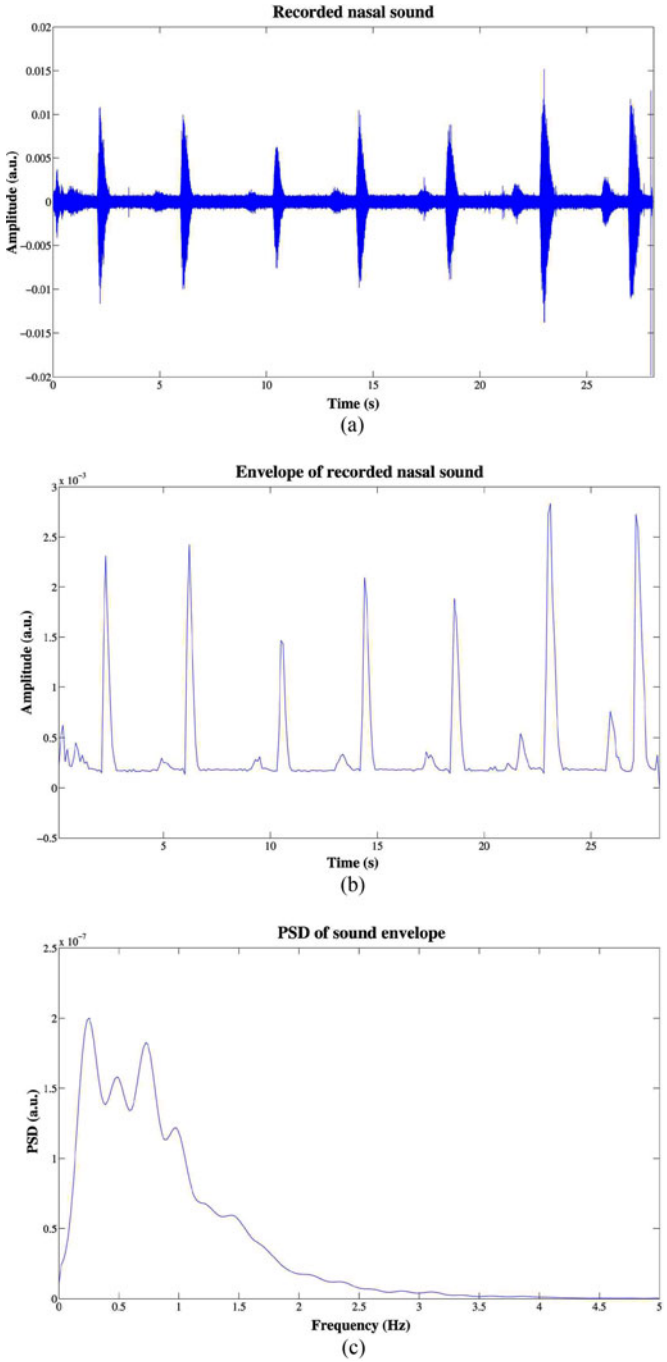

Fig. 7. Example of recorded nasal breath sound when the distance between the subject's nose and iPhone was 30 cm. (a) Filtered sound signal. (b) Downsampled envelope signal. (c) PSD of the envelope.

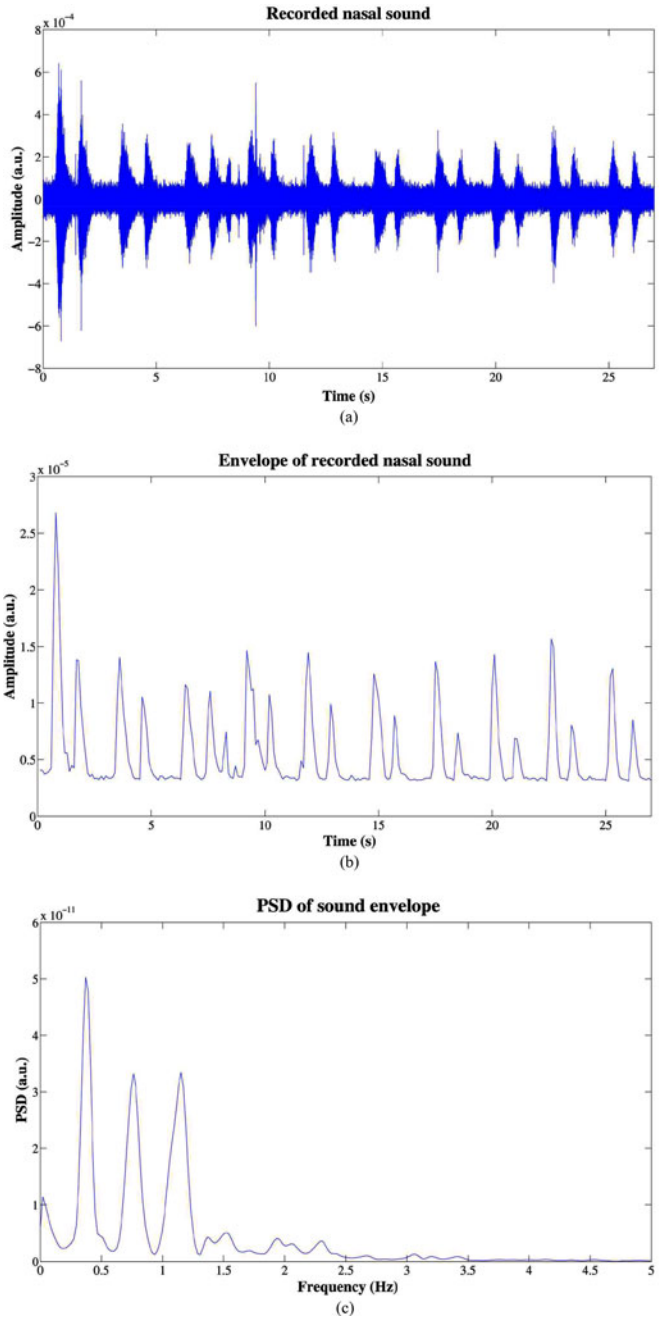

Fig. 8. Example of recorded nasal breath sound with background vocal noises when the distance between the subject's nose and iPhone was 30 cm. (a) Filtered sound signal. (b) Downsampled envelope signal. (c) PSD of the envelope.

IV. Discussion and Conclusion

In this paper, methods for estimating respiratory rate from tracheal and nasal breathing sound signals have been presented. Previously, our research group explored the feasibility of using a smartphone together with a specifically designed acoustical sensor to record tracheal sounds from which respiratory rates could be estimated [20]. In contrast, the feasibility of using smartphones together with their built-in and standard headset microphones for estimating respiratory rates was tested in this paper. Another motivation for this paper is based on several previous studies that showed that accurate respiratory rates, especially at low breathing rates, could be obtained from pulse oximeters, but the accuracy of this approach degrades above 30 breaths/min. Theoretically, the characteristics of the breathing sounds obtained from smartphones' microphones match the respiratory rate; thus, accurate respiratory rates can be obtained. Our results indicate that certainly for low and high breathing ranges ($0.1-1.5$ Hz), this is feasible from nasal breathing sounds

recorded from smartphone microphones. For 0.1 Hz, due to randomly occurring background noise or other noise during acquisition, RR estimation could not be reliably estimated. For reliable estimates of RR, the background noise should be kept at minimal which can be problematic for intensive care units.

We compared both Welch and AR spectra of the tracheal and nasal envelope sounds acquired with smartphones for respiratory rate estimation using the largest spectral peaks. Both spectral methods provided accurate respiratory rate estimation from nasal sounds in this study for both low and high breathing rates. However, for high breathing rates (0.8−1.5 Hz), a simple approach using the largest spectral peak detection could not always provide good results especially when subjects suffered from nasal congestion.

Microphone sensitivity is typically measured with a 1 kHz sine wave at a 94 decibels (dB) sound pressure level (SPL), or 1 pascal (Pa) pressure. The magnitude of the analog or digital output signal from the microphone with that input stimulus is a measure of its sensitivity. In this paper, the sound signals were obtained by an iPhone 4S that has two microphones, a Infineon 1014 microphone on top of the device and a Knowles S1950 microphone in the bottom [21]. The Infineon 1014 microphone is used for canceling out background noise, and it is located on the top of the unit near the headphone jack; the main microphone is on the bottom left [22]. All current iOS devices (iPhone 3GS and later, iPod touch 4 and later, and all iPads) include built-in microphones. However, Apple included a very steep high-pass filter, which presumably works as a wind and pop filter. The low-frequency roll-off for the internal microphone in these devices is very steep, on the order of 24 dB/octave starting at 250 Hz [23]. However, with the advent of the iOS 6, we are able to turn off the low-frequency roll-off filter, thereby resulting in fairly flat response [23]. Even though the performance of a smartphone is limited, we have compensated for these microphones as much as possible.

Better performance in detecting the Apnea–Hypopnea index or sleep apnea/hypopnea syndrome from the analysis of breath sounds recorded by a microphone of a smartphone can be achieved when combined with an oximetry signal. There have been efforts to monitor patients with asthma and chronic obstructive pulmonary disease [24], [25], with other severe respiratory diseases [26], and with nasal obstruction [27], however there have not been studies reporting respiratory rate estimation considering nasal congestion, to our knowledge. In this paper, the spectral morphology of nasal sound signals was analyzed to develop the respiratory rate estimation methods. The intensity changes of nasal sound signals were investigated to choose the best approach.

Since some people may feel some discomfort when they need to use an earpiece-microphone or placing a smartphone's microphone directly underneath their nose, a noncontact breathing sound acquisition has been conducted to illustrate that breathing rates can still be accurately derived even if a smartphone is 30 cm away from the nose. Certainly, this approach is more prone to background noise, however, provided that they are not overwhelming and mask the nasal breathing sounds, our approach appears to provide good respiratory rate estimates. A more thorough analysis under various background noise levels will need to be performed to augment our preliminary results on having a smartphone as far as 30 cm from the nose.

In summary, we have shown that the accurate RR can be estimated for nasal breathing sounds acquired from a smartphone's microphone as the estimation errors were less than 1% for cases considered in this paper. The fact that our approach does not require any external sensors, as all that is required is to place a smartphone's microphone underneath one's nose, is attractive from many perspectives. To date, with promising results obtained from this paper, smartphones can be used as a vital sign monitoring device that can readily provide heart rates and respiratory rates rather reliably without using any expensive external sensors. It is expected that future work by either our laboratory or others will result in additional vital sign capabilities directly from smartphones' or tablets' resident sensors.

REFERENCES

[1] M. A. Cretikos, R. Bellomo, K. Hillman, J. Chen, S. Finfer, and A. Flabouris, "Respiratory rate: The neglected vital sign," *Med. J. Australia*, vol. 188, no. 11, pp. 657–659, 2008.

[2] M. A. Peberdy, W. Kaye, J. P. Ornato, G. L. Larkin, V. Nadkarni, M. E. Mancini, R. A. Berg, G. Nichol, and T. Lane-Trultt, "Cardiopulmonary resuscitation of adults in the hospital: A report of 14 720 cardiac arrests from the National Registry of Cardiopulmonary Resuscitation," *Resuscitation*, vol. 58, no. 3, pp. 297–308, 2003.

[3] K. Reed *et al.*, "The Sixth Annual HealthGrades Patient Safety in American Hospitals Study," (2009, Apr.). [Online]. Available: http://www.mmhospital.org/upload/docs/Homepage/PatientSafetyInAmericanHospitalsStudy2009_Embargoed.pdf, Accessed Sep. 29, 2015.

[4] F. Q. Al-Khalidi, R. Saatchi, D. Burke, H. Elphick, and S. Tan, "Respiration rate monitoring methods: A review," *Pediatric Pulmonol.*, vol. 46, no. 6, pp. 523–529, Jun. 2011.

[5] K. Hillman, J. Chen, M. Cretikos, R. Bellomo, D. Brown, G. Doig, S. Finfer, A. Flabouris, and MERIT study investigators, "Introduction of the medical emergency team (MET) system: A cluster-randomised controlled trial," *Lancet*, vol. 365, no. 9477, pp. 2091–2097, 2005.

[6] Y. Nam, J. Lee, and K. Chon, "Respiratory rate estimation from the built-in cameras of smartphones and tablets," *Ann. Biomed. Eng.*, vol. 42, no. 4, pp. 885–898, 2014.

[7] G. Comtois, J. I. Salisbury, and Y. Sun, "A smartphone-based platform for analyzing physiological audio signals," in *Proc. 38th Annu. Northeast Bioeng. Conf.*, 2012, pp. 69–70.

[8] H. Pasterkamp, S. S. Kraman, and G. R. Wodicka, "Respiratory sounds: Advances beyond the stethoscope," *Amer. J. Respiratory Critical Care Med.*, vol. 156, no. 3, pp. 974–987, 1997.

[9] J. S. Chuah and Z. K. Moussavi, "Automated respiratory phase detection by acoustical means," in *Proc. 20th Annu. Int. Conf. Eng. Med. Biol. Soc.* 2004, pp. 21–24.

[10] P. Hult, B. Wranne, and P. Ask, "A bioacoustic method for timing of the different phases of the breathing cycle and monitoring of breathing frequency," *Med. Eng. Phys.*, vol. 22, no. 6, pp. 425–433, 2000.

[11] A. Kulkas, E. Huupponen, J. Virkkala, M. Tenhunen, A. Saastamoinen, E. Rauhala, and S.-L. Himanen, "Intelligent methods for identifying respiratory cycle phases from tracheal sound signal during sleep," *Comput. Biol. Med.*, vol. 39, no. 11, pp. 1000–1005, 2009.

[12] Z. K. Moussavi, M. T. Leopando, H. Pasterkamp, and G. Rempel, "Computerised acoustical respiratory phase detection without airflow measurement," *Med. Biol. Eng. Comput.*, vol. 38, no. 2, pp. 198–203, 2000.

[13] J. Cummiskey, T. Williams, P. Krumpe, and C. Guilleminault, "The detection and quantification of sleep apnea by tracheal sound recordings," *Amer. Rev. Respiratory Dis.*, vol. 126, no. 2, pp. 221–224, 1982.

[14] H. Nakano, M. Hayashi, E. Ohshima, N. Nishikata, and T. Shinohara, "Validation of a new system of tracheal sound analysis for the diagnosis of sleep apnea-hypopnea syndrome," *Sleep*, vol. 27, no. 5, pp. 951–958, 2004.

[15] A. Yadollahi and Z. M. Moussavi, "A robust method for estimating respiratory flow using tracheal sounds entropy," *IEEE Trans. Biomed. Eng.*, vol. 53, no. 4, pp. 662–668, Apr. 2006.

[16] M. Mahagnah and N. Gavriely, "Repeatability of measurements of normal lung sounds," *Amer. J. Respiratory Critical Care Med.*, vol. 149, no. 2, pp. 477–481, 1994.
[17] N. E. Huang, Z. Shen, S. R. Long, M. C. Wu, H. H. Shih, Q. Zheng, N.-C. Yen, C. C. Tung, and H. H. Liu, "The empirical mode decomposition and the Hilbert spectrum for nonlinear and non-stationary time series analysis," *Proc. Roy Soc. A, Math. Phys. Eng. Sci.*, vol. 454, no. 1971, pp. 903–995, 1998.
[18] S. Haykin, *Adaptive Filter Theory*, 2nd ed. Upper Saddle River, NJ, USA: Prentice-Hall, 1991.
[19] C.-L. Que, C. Kolmaga, L.-G. Durand, S. M. Kelly, and P. T. Macklem, "Phonospirometry for noninvasive measurement of ventilation: Methodology and preliminary results," *J. Appl. Physiol. (1985)*, vol. 93, no. 4, pp. 1515–1526, Oct. 2002.
[20] B. A. Reyes, N. Reljin, and K. H. Chon, "Tracheal sounds acquisition using smartphones," *Sensors*, vol. 14, no. 8, pp. 13830–13850, Jul. 2014.
[21] iFixit, "iPhone 4 Microphone Teardown," (2011, May). [Online]. Available: http://www.ifixit.com/Teardown/iPhone+4+Microphone+Teardown/3473, Accessed Sep. 29, 2015.
[22] Wikipedia, "iPhone 4S," (2015, Sep.). [Online]. Available: https://en.wikipedia.org/wiki/IPhone_4S, Accessed September 29, 2015.
[23] Faber Acoustical, "iOS 6 kills the filter on headset and mic inputs," (2012, Sep.). [Online]. Available: http://blog.faberacoustical.com/2012/ios/iphone/finally-ios-6-kills-the-filter-on-headset-and-mic-inputs, Accessed Sep. 29, 2015.
[24] M. Hasselgren, M. Arne, A. Lindahl, S. Janson, and B. Lundbäck, "Estimated prevalences of respiratory symptoms, asthma and chronic obstructive pulmonary disease related to detection rate in primary health care," *Scand. J. Prim. Health Care*, vol. 19, no. 1, pp. 54–57, 2001.
[25] D. C. Willems, M. A. Joore, J. J. Hendriks, R. A. van Duurling, E. F. Wouters, and J. L. Severens, "Process evaluation of a nurse-led telemonitoring programme for patients with asthma," *J. Telemed. Telecare*, vol. 13, no. 6, pp. 310–317, 2007.
[26] C. Maiolo, E. I. Mohamed, C. M. Fiorani, and A. De Lorenzo, "Home telemonitoring for patients with severe respiratory illness: The Italian experience," *J. Telemed. Telecare*, vol. 9, no. 2, pp. 67–71, 2003.
[27] H. Choi, I.-H. Park, H. G. Yoon, and H.-M. Lee, "Wireless patient monitoring system for patients with nasal obstruction," *Telemed. E-Health*, vol. 17, no. 1, pp. 46–49, 2011.

Author's photographs and biographies not available at the time of publication.